Research Journal of Cell Sciences

PRIME OPEN ACCESS

Volume 1, Issue 2

Research Article

Date of Submission: 10 June, 2025
Date of Acceptance: 07 July, 2025
Date of Publication: 25 July, 2025

Decorated BN Nanocones as NLO-Active Nanocarriers of Nitrosourea Anticancer Drug: A DFT Study

Maryam Souri*

Chemistry Department, College of Sciences, Payame Noor University, Iran

***Corresponding Author:** Maryam Souri. Chemistry Department, College of Sciences, Payame Noor University, Iran.

Citation: Souri, M. (2025). Decorated BN Nanocones as NLO-Active Nanocarriers of Nitrosourea Anticancer Drug: A DFT Study. *Res J Cell Sci, 1*(2), 01-14.

Abstract

Nonlinear optical (NLO) materials are rapidly gaining attention due to their broad potential for various technical applications. In this research a group of decorated Boron Nitride nanocones (BNNCs) have been introduced as potential NLO active drug carriers. DFT study of the electronic structure of BNNCs indicates that Zn- and Mg-decorated BNNCs can serve as nanocarriers for the anticancer agent Nitrosourea (NU). These structures undergo a significant alteration in their electronic properties when they bond with NU. This renders them highly suitable for therapeutic and diagnostic applications. TD-DFT analysis confirms the red shift in UV-Vis absorption peaks of BNNCs due to complex formation with NU. Moreover, results demonstrate the impact of band gaps on different linear and nonlinear optical properties of BNNCs.

Keywords: Nonlinear Optical Materials, BN Nanocones, DFT, Nitrosourea, Drug Delivery

Introduction

Finding new nonlinear optical (NLO) materials is demanding in different areas of optical signal processing, optical communication, ultrafast photonics, optical switching, data storage, holographic imaging, telecommunications, and optical switches [1-6]. Various organic, inorganic, and organo-metallic NLO materials have been explored in research [7-9]. Small NLO active organic molecules are not ideal for practical use due to their low stability, while inorganic materials offer higher mechanical strength and stability [10, 11].

Recently, NLO active materials have been extensively studied theoretically [6, 12-15] and experimentally [1, 16-20]. Scientists have tried diverse methods to enhance the NLO activity of inorganic and organic materials. Utilizing donor-acceptor bridges, extended π conjugation, and designing metal-ligand frameworks based on charge transfer from the metal to the ligand [21, 22], push-pull effects [23], and introducing excess electrons [3, 4] are some of these strategies. Among these methods, using excess electrons is a popular choice, providing benefits such as impressive charge transfer and reduced energy of transition. Doping alkaline earth metals, alkali metals, and transition metals are commonly used to introduce excess electrons into molecules and enhance the NLO response [24].

In recent decades, various types of nanostructure have been widely utilized as sensors and drug carriers [25-32]. High selectivity, improved absorption, decreased side effects, and low drug toxicity are significant advantages of drug nanocarriers [33-35]. The rapid growth of nanotechnology in the past few years has sparked innovative ideas and approaches for treating and diagnosing diseases that were previously untreatable [36]. Utilizing nanostructures to deliver drugs solves several issues in traditional drug delivery methods, such as low solubility, short duration of effectiveness, toxicity, abrupt release, difficulty in absorption, and compatibility with the body [37]. This has revolutionized the field of medicine by providing a way to maintain the effectiveness of medications while minimizing side effects.

Nitrosourea (NU), CH3N3O2, is an anticancer drug capable of treating different malignancies, including solid tumors, brain tumors, leukemia, lymphomas, and Hodgkin's disease [34, 38-40]. Nitrosourea inhibits the DNA repair mechanisms of cancer cells through the alkylation process. As a result, it causes DNA damage and cellular death [41]. However, severe

side effects, including pulmonary fibrosis, myelosuppression, neurotoxicity, bone marrow suppression, nausea, vomiting, hepatotoxicity, nephrotoxicity, and ocular toxicity, significantly limit the use of this drug [34]. Different nanostructures, including nanocages graphene nanoribbons nanosheets, nanoclusters monolayers and two-dimensional system have been previously introduced as successful nitrosourea carriers [39, 42-51].

BN nanostructures are characterized by exceptional structural and chemical stability, excellent oxidation resistance, and remarkable mechanical properties [52]. These qualities make the BN family a promising option for various technical uses. The semi-ionic nature of the B-N bond, due to the difference in electronegativity between Nitrogen and Boron atoms, allows for electrophilic or nucleophilic interactions at each Nitrogen or Boron atom in BN nanostructures [53-55]. It has shown that the characteristics of the BN nanocones, produced by rolling BN nanosheets, vary based on the specific segment deleted from the original nanosheet [56]. Recent advancements in nanotechnology have highlighted the potential of boron nitride (BN) nanotubes as effective nanocarriers for anti-cancer drugs. Makiabadi et al. introduced BN nanotubes specifically for the delivery of Azacitidine and Decitabine [57]. In a complementary study, Aiswarya et al. employed density functional theory (DFT) to evaluate boron carbon nitride nanocages and boron nitride nanosheets as carriers for the melphalan drug, further underscoring the versatility of BN materials in drug delivery applications. Additionally, Saadh et al. utilized DFT estimations to investigate the interactions between BN-biphenyl nanosheets and the anti-cancer drug 5-fluorouracil (5-FU), revealing insights into the binding mechanisms that could enhance therapeutic outcomes. BN nanocones have been employed as detectors and biosensors because of their absorption capacity [27,58-61]. Additionally, their non-toxicity and biocompatibility make BN nanostructures suitable for medical applications, mainly as nanocarriers [52]. Combining a drug's medical effects with the nonlinear optical properties of a drug-carrier complex could lead to the development of theranostic agents. One of the well-known nonlinear optical operations is second harmonic generation, where a light wave passing through a nonlinear material changes to a wave with double its frequency [62]. This process allows for operation in electromagnetic spectrum regions that are usually not reachable. NLO materials play a significant role in advancements in medicine, such as the development of bioimaging and photonic lasers [63-65].

The electronic properties and optical feature of B17N18H15 nanocone ond some of its derivatives have been studied in our previous work and Ni- Decorated nanocone has been introduced as the most hopeful NLO active nanocarrier [66]. In this research, a group of decorated B17N18H15 nanocones have been considered NLO active nanocarriers of nitrosourea anticancer drug. The role of doped elements on the electronic characteristics of nanocones has been studied. Also, different optical properties of nanostructures have been traced before and after complexation with NU.

Asif et al. conducted research on the nonlinear optical (NLO) response of π-conjugated polyaromatic hydrocarbons, revealing that the optical efficiency of these structures is enhanced through doping with super halogens. In another study, Rashid et al. demonstrated improved NLO response of boron phosphide nanosheets due to alkali metal doping. Yaghoob et al. further investigated the enhancement of NLO properties in silicon carbide nanosheets resulting from similar alkali metal doping [6,9,67]. Additionally, Rasool et al. utilized gold doping to boost the NLO performance of graphyne [68]. In the current research, metal decoration has been employed as a strategy to improve both the absorption capacity and NLO activity of B17N18H15 nanocones, focusing on their electronic properties and optical features as potential NLO-active nanocarriers for the nitrosourea anticancer drug.

Computational Method

The B3LYP functional is recognized for its ability to efficiently and accurately calculate the electronic properties of wide range of materials [69, 70]. In previous studies on Boron Nitride systems the B3LYP functional has been used commonly [71-76]. In this study, calculations were conducted using the B3LYP hybrid DFT functional and def2-SVP basis set. The polarizability and hyperpolarizability of nanostructures were considered through static frequencies. UV-vis spectra and pertaining electronic transitions were computed in TD-B3LYP/def2-SVP level of theory. The electronic characteristics of nanocones were further understood by analyzing the frontier molecular orbitals (FMOs) and density of states (DOS) diagrams. The Gaussian 09 program package was employed for all calculations. Moreover, GaussSum 3.0 was used to visualize UV-vis spectra and DOS diagrams [77,78].

Results and Discussion

Frontier Molecular Orbital (FMO) Analysis

Nanocones, characterized by their disclination angle, are cone-shaped structures. When a flat sheet transforms into a cone shape, a section of the sheet must be removed in order to form the cone. The size of this section is determined by the disclination angle. The disclination angle of all Boron Nitride nanocones (BNNCs) considered in this study is 60°. To minimize boundary effects, the ends of the BNNCs were saturated with Hydrogen atoms. The optimization of the nanostructures was carried out without imposing any symmetry constraints. Figure 1 summarized the structure of studied decorated BNNCs and NU agent.

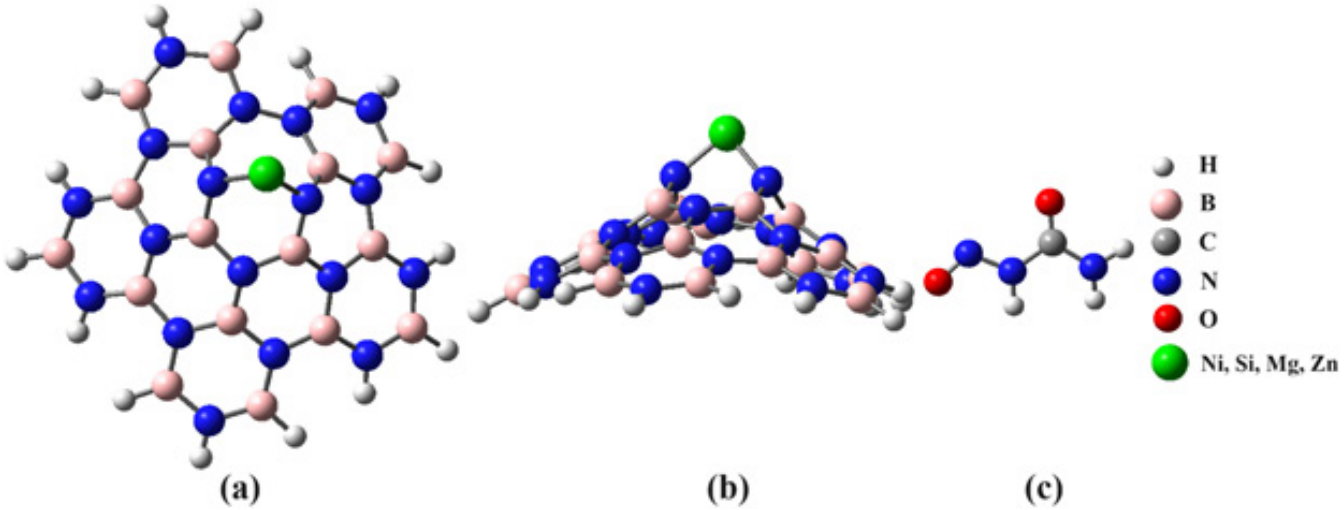

Figure 1: a) and b) the general structure of considered decorated BNNCs (including Mg-BNNC, Si-BNNC, Ni-BNNC, Zn-BNNC), top view, and side view, respectively. c) optimized structure of anticancer agent, Nitrosourea (NU)

Understanding the electronic structure and reactivity of molecules can be aided by considering their frontier molecular orbitals (FMOs). FMO analysis is a valuable tool for assessing the efficiency of charge transport within a molecule. Figure 2 summarizes the Highest Occupied Molecular Orbital (HOMO) and Lowest Unoccupied Molecular Orbital (LUMO) of the considered nanocones. HOMOs of all nanostructures are located around the doping area. Comparatively, LUMOs are more concentrated on the doping position. Based on it, this area of the molecule is recognized as a potential intermolecular interaction site. This region is ready to bond to the NU molecule.

Based on the energy of FMOs, indicated in Figure 2, the band gaps, Eg, have been calculated and mentioned in this figure. The lowest Eg belongs to Zn-BNNC. The Eg of Mg-BNNC is almost the same as Zn-BNNC. Si-BNNC and Ni-BNNC are in the following ranks, respectively.

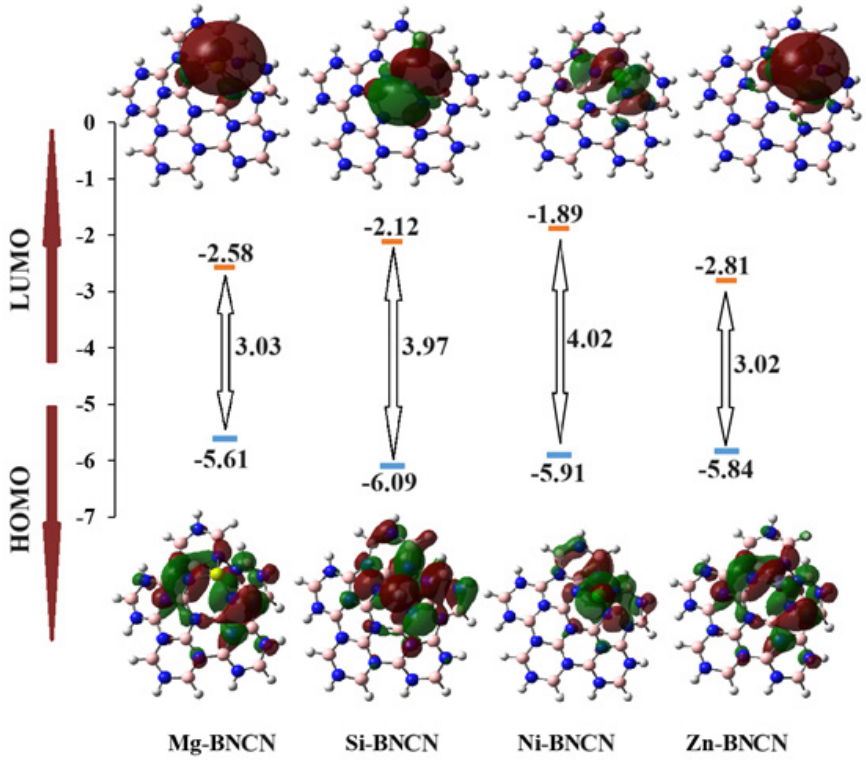

Figure 2: The FMOs profiles of the decorated BNNCs. Related energies and band gaps (in eV) have been mentioned, too

Figure 3 illustrates the density of states (DOS) profiles for the considered nanostructures. DOS analysis provides insights into the electron density distribution within the frontier molecular orbitals (FMOs) and helps understand electronic transitions. Examination of the DOS diagrams reveals a consistent pattern across all nanocones. Notably, the DOS is lower near the active orbitals involved in molecular interactions, specifically the FMOs.

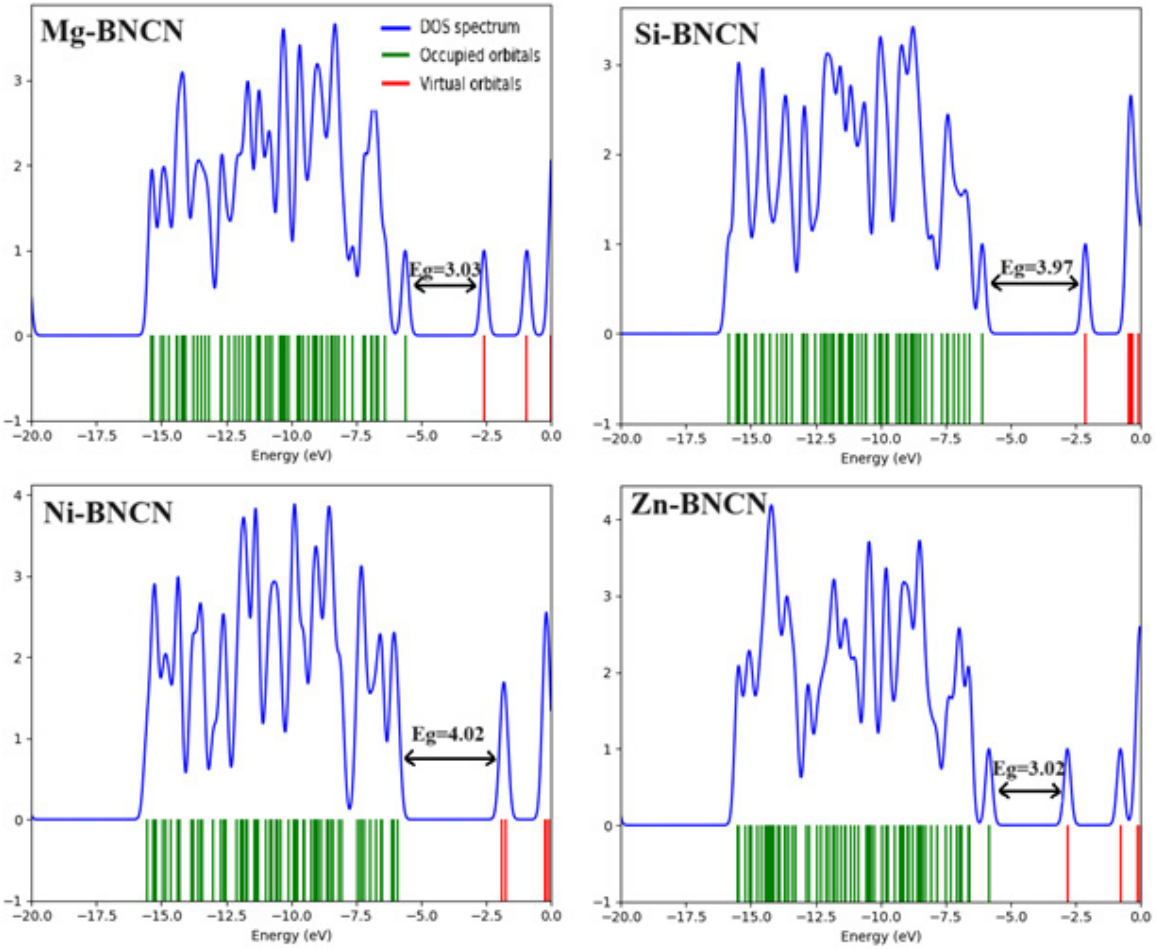

Figure 3: The DOS diagrams of studied BNNCs

Global reactivity descriptors like Fermi energy level (E_{FL}), ionization potential (IP), electron affinity (EA), chemical hardness (h), and global softness (s) are dependent to the E_g. Table 1 summarized the Global reactivity descriptors of considered BNNCs. The total energies of nanocones are indicated in this table, too.

The higher E_g, corresponds to a lower charge transfer probability. Consequently, it lessen the chemical reactivity, and enhance the kinetic stability [79]. With the most significant band gap, Ni-BNNC is predicted to be the most stable nanocone studied and, correspondingly, the least reactive. Si-BNNC shows almost the same measure of stability. Also, two other nanocones Mg-BNNC and Zn-BNNC almost equally have the least stability (the most remarkable chemical reactivity). The Fermi energy level (E_{FL}) represents the thermodynamic work required to add an electron to a molecule. It is typically approximated as the midpoint of the band gap [80]. The minimum Fermi energy belongs to Zn-BNNC. E_{FL} increases gradually in Si-BNC, Mg-BNC, and Ni-BNC, respectively.

The ionization potential (IP) is a measure of the amount of energy required to excite electrons from the HOMO. At the same time, EA is the energy released during the placement of an electron in the LUMO. In other words, the ability to accept and donate electrons by a molecule is described by EA and IP values, respectively. Greater chemical stability of a substance is indicated by higher IP values. According to Koopman's theorem the negative of the HOMO energy is considered as IP [81]. Conversely the negative of the LUMO energy is considered as EA [82, 83]. IP decreases in this trend: Si-BNNC, Ni-BNNC, Zn-BNNC, and Mg-BNNC. On the other hand, Zn-BNNC has the greatest EA. Mg-BNNC, Si-BNNC, and Ni-BNNC are in following ranks, respectively.

The chemical hardness (h) indicates the amount of charge transfer in a molecule. It could be calculated as $\frac{IP-EA}{2}$ [81]. Intramolecular charge transfer enhances the chemical stability of a molecule and consequently reduces the chemical reactivity. In other words, increased hardness causes more kinetical stability [82]. The global softness (s) is defined as $\frac{1}{\eta}$. Hardness alterations is totally in agreement with E_g trend. Having the greatest E_g, Ni-BNNC shows the highest hardness (and the least softness). It is expected to show the minimum chemical reactivity. Si-BNNC, Mg-BNNC, and Zn-BNNC are in the following ranks, respectively. The softness of considered nanostructures decrease in trend: Mg-BNNC≈ Zn-BNNC>Si-BNNC≈Ni-BNNC.

Molecule	Total energy	E_{FL}	IP	EA	h	s
Mg-BNNC	-1617.73	-4.10	5.61	2.58	1.52	0.66
Si-BNNC	-1707.13	-4.11	6.09	2.12	1.99	0.50
Ni-BNNC	-2925.86	-3.90	5.91	1.89	2.01	0.50
Zn-BNNC	-3196.85	-4.32	5.84	2.81	1.51	0.66

Table 1: Total energy (in a.u.), Fermi energy level (EFL), ionization potential (IP), electron affinity (EA), Chemical hardness (h), and Global softness (s) (in eV) of modified BNNCs

Optical Properties

There are different criteria to describe the optical properties of a molecule, Including average polarizability (α), first-order hyperpolarizability (β) and second-order hyperpolarizability (γ). When a molecule is exposed to a weak, uniform electric field, the energy of the molecule depends on the electric field's intensity. The energy expansion in terms of the Taylor series is as follows:

$$E = E^0 - \mu_i F_i - \frac{1}{2}\alpha_{ij}F_iF_j - \frac{1}{6}\beta_{ijk}F_iF_jF_k - \frac{1}{24}\gamma_{ijkl}F_iF_jF_kF_l - \cdots \qquad \text{(eq. 1)}$$

E^0 is the molecule's energy in the absence of an electronic field and E is the energy of the perturbed condition. μ_i is the component of the dipole moment? F_i is the component of field strength? α_{ij}, β_{ijk} and γ_{ijkl} are the components of polarizability, first-order hyperpolarizability, and second-order hyperpolarizability, respectively [83] .

In this study, different optical parameters have been calculated using the DFT computational method. μ, α_0, α, β, and γ of NU, and different BNNCs have been summarized in Table 2. It is important to note that the primary focus of this work is the qualitative comparison of NLO properties across different nanocone structures. Therefore, the absolute values of hyperpolarizability should be interpreted with caution. Utilizing higher-level computations, such as the M06 and PBE0 methods and the def2-TZVP basis set, may provide a more accurate representation of the electronic characteristics of the nanostructures under consideration

Molecule	μ	α_0	α	β	γ
NU	5.72	37.75	33.39	69.45	3970.53
Mg-BNNC	5.35	318.10	125.86	875.71	105680.00
Si-BNNC	2.09	322.70	156.59	4.78	56684.10
Ni-BNNC	1.40	327.63	156.61	763.76	77214.20
Zn-BNNC	3.04	318.29	130.83	375.80	78608.00

Table 2: μ (in Debye), α_0, α, β and γ (in au) of studied BNNCs

The dipole moment indicates the net polarity of the molecule. As mentioned in Table 2, Ni decorated nanocone has the least polarity among considered nanocones. μ increases in this order: Si-BNNC, Zn-BNNC and Mg-BNNC. Doping cause kind of torsion on the structure of BNNC. The amount of this torsion is different in various considered nanocones. It causes such a variation in μ values of them.

The α_0 of studied nanocones are so close together. There are less than 5% difference between them. α of the nanocones don't show considerable difference, too. However, Si-BNNC and Ni-BNNC have the maximum amount of α. Their α value is almost the same, 156.6 au. The first and second hyperpolarizability are nonlinear optical properties of a material. The NLO activity of a molecule is described in terms of its β and γ values. There are significant differences between β and γ amounts of BNNCs. Mg-BNNC has the highest β value, about 876 au. After that, Ni-BNNC, Zn-BNNC, and Si-BNNC are in the next orders, respectively. Mg-BNNC has the highest γ value, too. Ni-BNNC and Zn-BNNC have almost similar γ values. Si-BNNC shows the least γ value.

Molecular Electrostatic Potentials

Molecular Electrostatic Potential (MEP) profiles provide a clear insight into the distribution pattern of electrostatic charges at the surface of the molecule. By identifying the nucleophilic and electrophilic regions of the molecule, MEP facilitates the study of molecular reactivity. In the MEP diagram, the blue areas represent electron poverty and propensity for nucleophilic attack. On the other hand, the red areas indicate electron accumulation and electrophilic attack tendency. The MEP profiles of doped BNNCs and NU are shown in Figure 4.

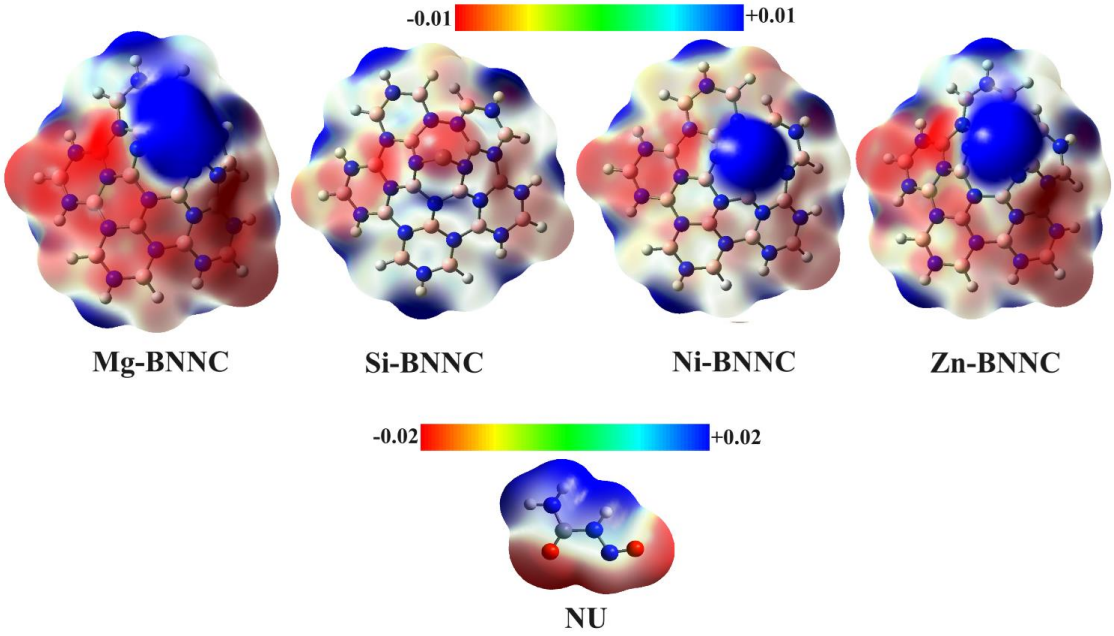

Figure 4: The MEP profiles of studied nanostructures. The shift from red to blue indicates a change from areas of high electrical potential to low electrical potential

According to the MEP maps, the metal-doped BNNCs show a significant electrophilic area around the doping position. However, the Si-BNNC doesn't have such an area. In other word all considered BNNCs except Si-BNNC are expected to get involved in an intermolecular interaction with a nucleophile species. On the other hand, NU molecule has an electron reach area in a side contains two Oxygen atoms and a Nitrogen. It seems that NU can attack to the BNNCs via this area.

NU Absorption by BNNCs

One of the critical hurdles in developing intelligent drug delivery systems is identifying a suitable carrier that does not compromise the integrity and efficacy of the medication. The ideal carrier should have a structure that allows some of its properties to change when it binds to the drug, enabling the ability to monitor the drug's whereabouts in the body through detection methods. This study explores the potential of four BNNCs, for delivering the anticancer agent, NU. The optimized structure of these complexes is illustrated in Figure 5. Crucial atomic distances have been mentioned in this figure, too. To clarify the structures, they have been shown in two viewpoints.

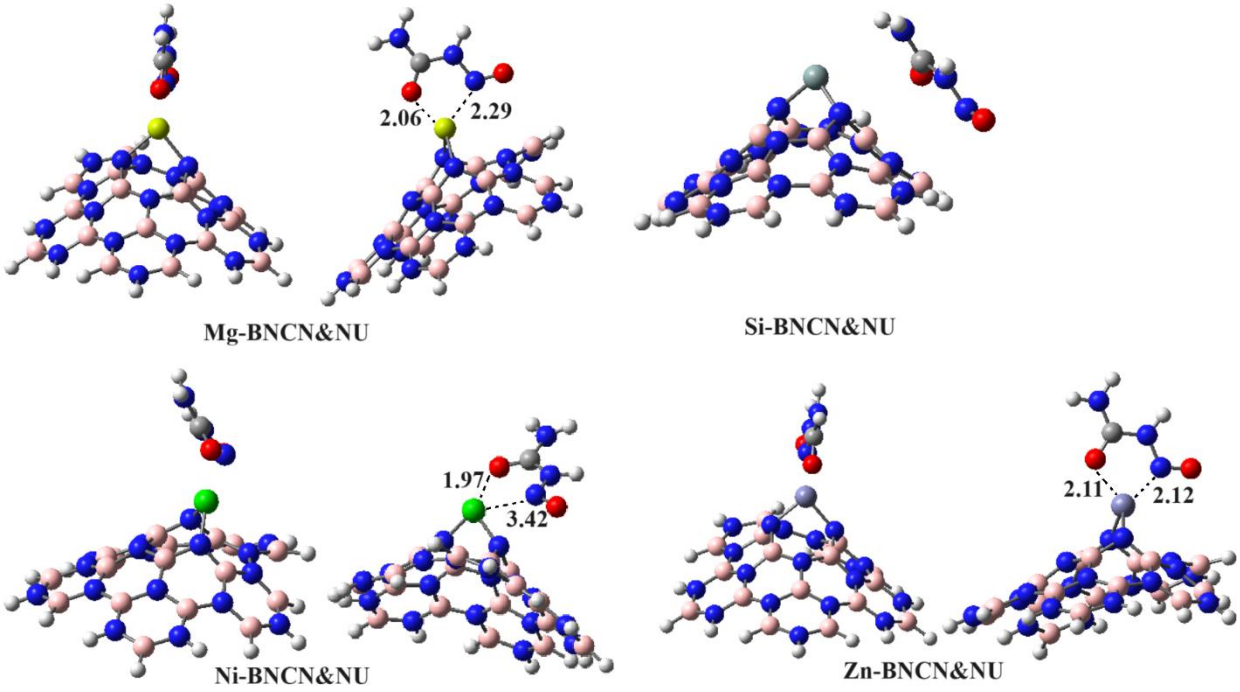

Figure 5: The optimized structure of NU&BNNCs. Distances are in Å

The interaction of Si-BNNC with NU is a weak, side to side one. In other complexes, O atom in CO group of NU interacts effectively with the doping atom. The shortest O-X (X=Mg, Ni, and Zn) distance belongs to Ni-BNNC&NU (1.97Å). Mg-BNNC&NU is in the next rank. Finally, the O-Zn distance is 2.11 Å.

The interactions between the Nu molecule and nanocone have been studied using a theoretical framework at the B3LYP/ def2-SVP level.

The drug-nanocone adsorption energy has been calculated to be:

$$E_{ad} = E_{NU\&nanocone} - (E_{nanocone} + E_{NU}) \quad \text{(eq. 10)}$$

Where, $E_{NU\&nanocone}$, $E_{nanocone}$ and E_{NU} are the total energy of NU&nanocone complex, nanocone, and NU, respectively. The energy of adsorption of NU on different BNNCs has been calculated and summarized in Table 3. (Total energies of NU and BNNCs are mentioned in Table 1.) Higher adsorption energy indicates stronger binding between the nanocone and the drug molecule. Mg-BNNC showed the highest adsorption energy, making it a promising candidate for NU delivery. Zn-BNNC&NU, Ni-BNNC&NU, and Si-BNNC&NU is in the next order of E_{ad}, respectively. The small amount of E_{ad} in Si-BNNC&NU complex agrees with the side to side interaction of Si-BNNC and NU, shown in

Figure 5; Also, the global reactivity descriptors predict this, well

	Mg-BNNC&NU	**Si-BNNC&NU**	**Ni-BNNC&NU**	**Zn-BNNC&NU**
Total energy	-1972.08	-2061.42	-3280.19	-3551.20
E_ad	-40.39	-4.84	-26.98	-38.48

Table 3: Total energy of NU&BNNCs (in a.u.) and absorption energies (in kcal/mol)

FMO energies of considered drug-nanocone complexes and different global reactivity descriptors have been summarized in Table 4. % ΔE_g in this table is the decreased percentage of band gap as a result of complex formation. It has been calculated as: $\%\Delta E_g = \frac{E_g^{BNNC} - E_g^{NU-BNNC}}{E_g^{BNNC}} \times 100.$

Molecule	**E_{HOMO}**	**E_{LUMO}**	**E_g**	**$\%\Delta E_g$**	**E_{FL}**	**EA**	**h**	**s**	**IP**
Mg-BNNC&NU	-4.65	-3.94	0.71	76.52	-4.30	3.94	0.36	2.81	4.65
Si-BNNC&NU	-5.99	-2.08	3.91	1.58	-4.03	2.08	1.95	0.51	5.99
Ni-BNNC&NU	-5.29	-2.77	2.52	37.22	-4.03	2.77	1.26	0.79	5.29
Zn-BNNC&NU	-4.86	-3.67	1.19	60.69	-4.26	3.67	0.59	1.68	4.86

Table 4: E_{HOMO}, E_{LUMO}, Band gap (Eg), Fermi energy level (E_{FL}), electron affinity (EA), Chemical hardness (h), Global softness (s), ionization potential (IP), (in eV), and % ΔE calculated for different NU&BNNCs

A significant alteration in the band gap after drug adsorption facilitates traceability through optical methods. Results show that complexation causes the band gap of all considered species to decrease. Mg-BNNC&NU and Zn-BNNC&NU exhibit the most substantial band gap changes compared with correlated bare nanocone, enhancing their suitability for theranostic applications. % ΔE_g of two other complexes decrease in this order: Ni-BNNC&NU, and Si-BNNC&NU. As global reactivity descriptors are dependent on E_g, their values are differing in single nanocones and drug- nanocones states. For the sake of simplicity comparison of global reactivity descriptors have been visualized in BNNCs have higher h and IP and lower EA and s, compared with NU-BNNCs. Mg-BNNC and Ni-BNNC have higher E_{FL} compared with related complexes with NU. However, Si-BNNC and Zn-BNNC have lower E_{FL}. Among considered nanocones Mg-BNNC shows more significant difference in single and complex forms.

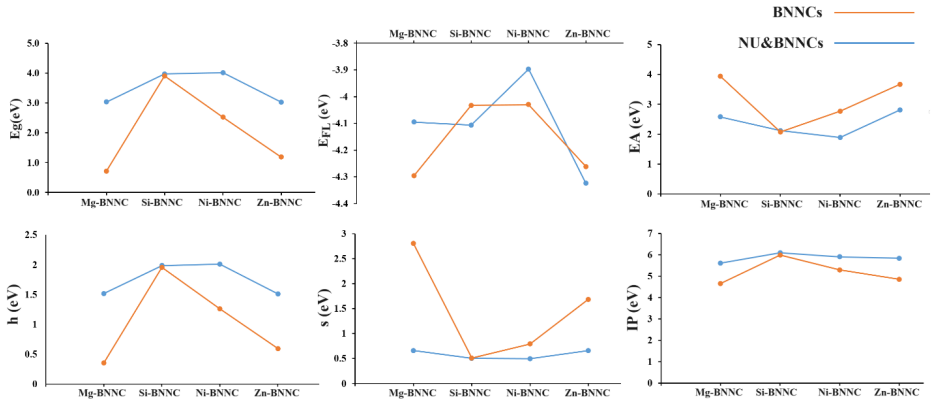

Figure 6: Comparison of global reactivity descriptors of Single BNNCs and NU&BNNCs.

μ, α_0, α, β, and γ of different NU-BNNCs has been summarized in Table 5. Si containing complex show the least dipole moments. Three other complexes have considerable dipole moments. The maximum μ belongs to Mg-BNNC&NU. The same trend is seen in $\boldsymbol{\alpha_0}$ data. $\boldsymbol{\alpha_0}$ values alter in the range of 361.22 (for Si-BNNC&NU) and 466.46 (for Mg-BNNC&NU). Unlike other properties in Table 5, the lowest value of α belongs to Ni-BNNC&NU. Zn-BNNC&NU, Si-BNNC&NU, and Mg-BNNC&NU is in the next orders, respectively. Studied complexes don't show considerable α values. The first hyperpolarizability of complexes alters from 200.78 au, for Si-BNNC&NU, to 4147 au, for Zn-BNNC&NU. The β value of Mg-BNNC&NU is close to Zn-BNNC&NU's. γ alteration is according to this trend: Ni-BNNC&NU> Mg-BNNC&NU > Zn-BNNC&NU > Si-BNNC&NU.

	μ	α_0	α	β	γ
Mg-BNNC&NU	15.29	446.46	201.27	4012.60	175718.00
Si-BNNC&NU	3.34	361.22	153.10	200.78	75440.10
Ni-BNNC&NU	10.33	376.77	127.87	2429.69	207879.00
Zn-BNNC&NU	13.35	420.67	148.17	4147.46	76293.20

Table 5: μ (in Debye), α_0, α, β, and γ (in au) of studied 5-NU&BNNCs

In order to clarify the effect of complexation with drug, the comparison of different optical properties of nanocones in a single form and complex with NU molecule have been summarized in Figure 7. The graphs show that, interaction with NU drug enhances μ and β of Si-BNNC partially and other BNNCs sharply. Both parameters were markedly higher for Mg-BNNC and Zn-BNNC upon drug adsorption, indicating their potential for monitoring drug delivery. α_0 of all nanocones increase as a result of complexation. Interaction with NU does not make considerable alteration in α values. However, Mg-BNNC is an exception. Complexation enhances its α value, significantly. Mg-BNNC and Ni-BNNC show a significant increase in γ after complex formation. However, γ of two other nanocones don't change considerably by interaction with drug molecule.

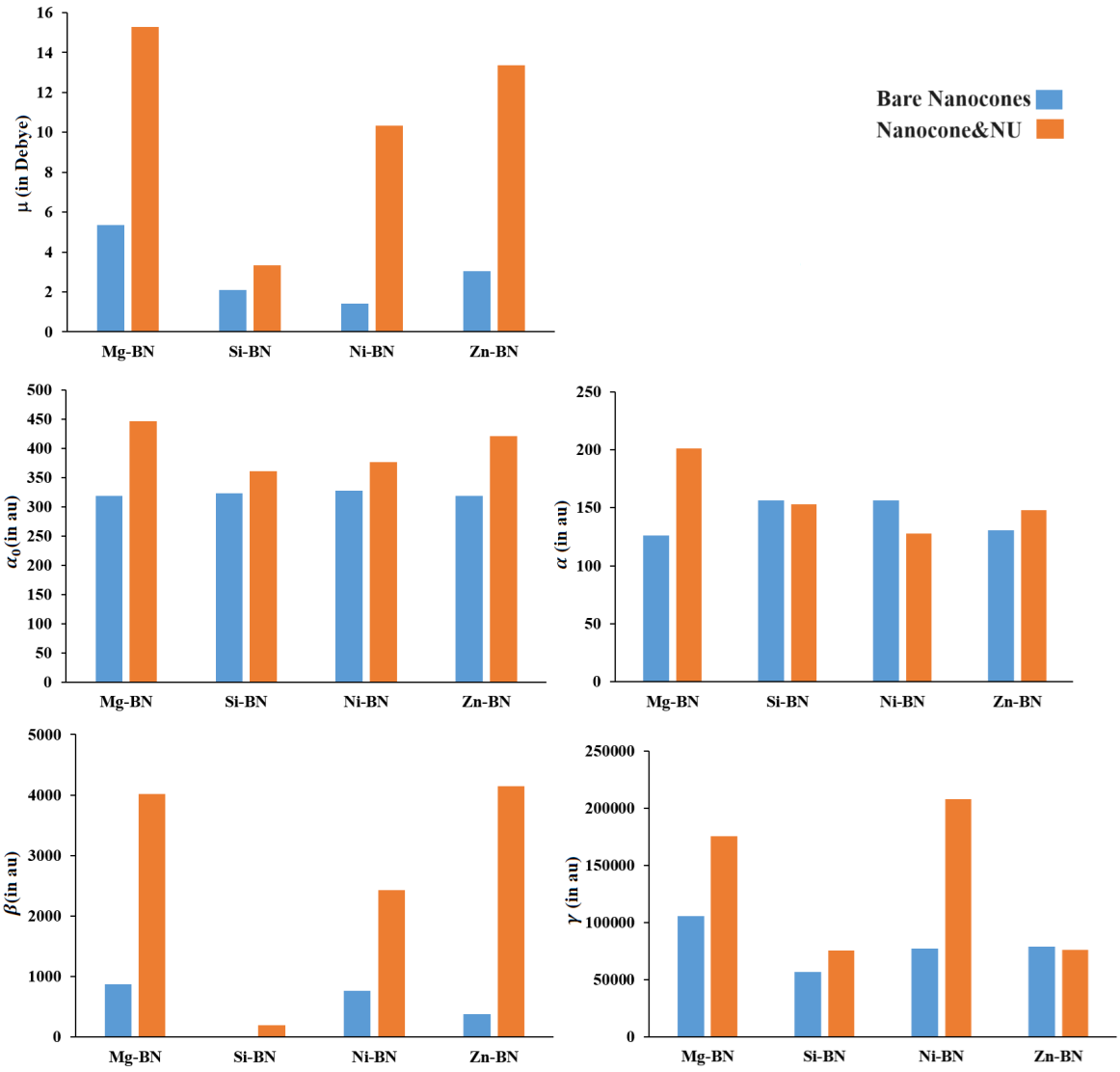

Figure 7: The comparison of μ, α_0, α , β, and γ of nanocones in the single form and complex with NU

As mentioned before, the FMO energies and resulting band gaps affect the linear and nonlinear optical properties of materials. A small energy gap between the ground state and excited state suggests that it is relatively easy for an electron to jump from its current state to a higher energy state. This ease of excitation is thought to lead to significant electron transfer, likely to result in a robust optical response.

As shown in Figure 8. a good correlation has been found between energy gap of BNNCs (in single and complex with NU) and μ, α_0 and β. The decrease of the E_g is accompanied with increase in μ, α_0 and β. However, no meaningful correlation has been seen between E_g and α or γ.

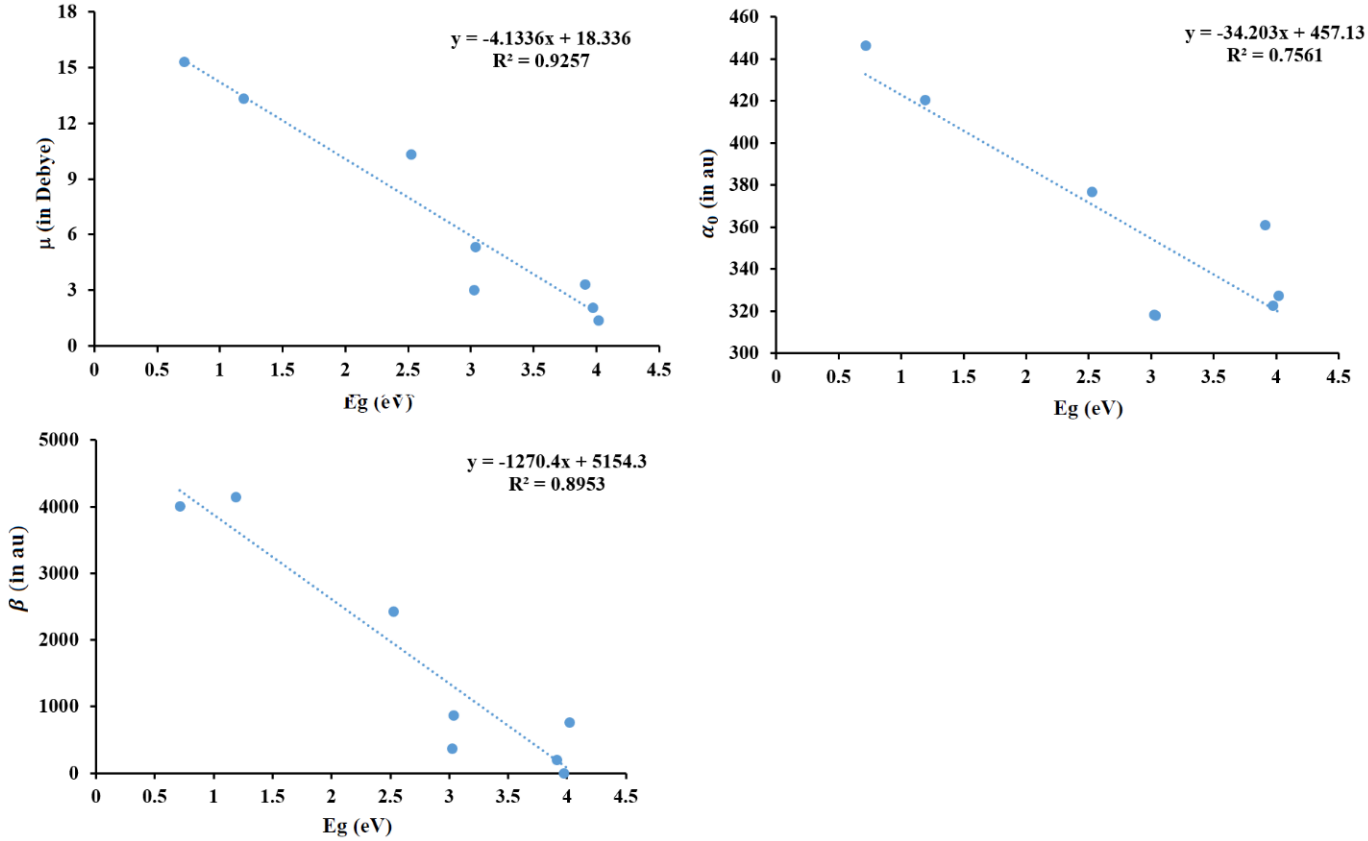

Figure 8: The correlation between optical properties (μ, α_0 and β) of BNNCs and relate band gaps (E_g)

Absorption Analysis

To investigate the absorption features of doped systems, an ultraviolet-visible (UV-Vis) study has been conducted. A common and effective method for analyzing the absorption spectra, excitation energy, and oscillator strength of molecules is time-dependent analysis. While the long-range corrected DFT methods often provide more accurate estimates of electronic excitations of systems where charge-transfer interactions or extended conjugation play a significant role TD-B3LYP is widely used because of low cost and fair efficiency [84-87]. Using time-dependent density functional theory (TD-DFT), we have calculated and listed in Table 6 the dominant transition energies, excitation energies, oscillator strengths (f_0) and wavelengths of maximum absorption (λ_{max}). This table reveals notable contributions to each electronic transition. Also, the UV-Vis absorption spectra of each BNNC and its complex with the NU molecule have been visualized in Figure 9.

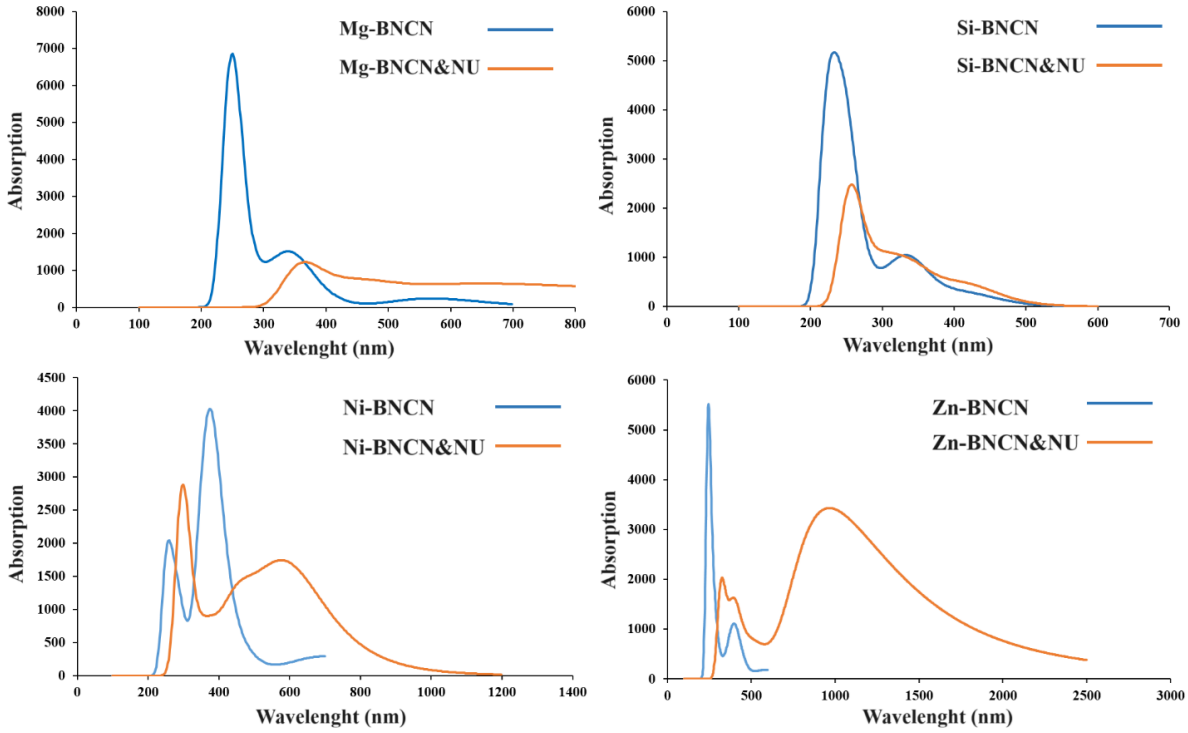

Figure 9: UV-vis absorption spectra of BNNCs in single form and complex with NU

All considered BNNCs show sharp UV-Vis absorption peaks in the UV region. Mg-BNNC has the most absorption intensity. The excitation energy responsible for this peak is 4.86eV. The related oscillator strength is 0.04. Zn-BNNC, Si-BNNC, and Ni-BNNC are in the following orders, respectively. Excitation energies of BNNCs are between 3.05 and 5.2 eV. The oscillator strength, f_{osc}, quantifies the likelihood of absorption occurring. Oscillator strength of BNNCs alter in the range of 0.01 and 0.08.

Absorption intensity decreases significantly as a result of complexation with the NU molecule. A red shift in absorption is observed in all complexes compared to their corresponding BNNCs. A comparable red shift has been previously reported due to the adsorption of drugs onto BN nanomaterials [88, 89]. The maximum absorption of Mg-BNNC&NU and Si-BNNC&NU happen in the UV region. Ni-BNNC&NU has a sharp UV-Vis absorption peak in the UV area and a broad one in the visible region. Zn-BNNC&NU shows a peak having low absorption intensity in visible area and a broad high intensity one in near infrared (NIR) region. For NU-BNNCs λ_{max} alters between 258.65 and 895.37, and f_{osc} is between 0.01 and 0.06. All in all, NU-BNNCs show lower excitation energies and less probability of absorption compared with their relative BNNCs.

	ΔE (eV)	λ_{max} (nm)	f_{osc}	Major contributions
Mg-BNNC	3.58 4.86	346.76 255.14	0.01 0.04	H-3→L (68%) H-1→L+1 (59%)
Mg-BNNC&NU	3.47	357.30	0.01	H-13→L (39%), H-12→L (32%)
Si-BNNC	3.64 5.03	340.95 246.29	0.02 0.04	H-1→L (81%) H→L+3 (87%)
Si-BNNC&NU	4.79	258.65	0.03	H→L+2 (73%)
Ni-BNNC	3.32 4.95	373.03 250.38	0.08 0.03	H-2→L+1 (81%) H-8→L+1 (58%)
Ni-BNNC&NU	2.08 4.13	595.04 299.88	0.02 0.05	H-2→L (88%) H-5→L+1 (65%)
Zn-BNNC	3.05 5.20	406.61 238.18	0.02 0.03	H-1→L (69%) H-1→L+1 (51%)
Zn-BNNC&NU	1.38 3.11	895.37 398.32	0.06 0.03	H-1→L (75%) H-8→L (95%)

Table 6: Excitation energy (ΔE in eV), maximum absorption wavelength (λmax in nm), highest oscillator strength (fosc), and transitions with significant contributions for BNNCs and their complexes with NU. (H is HOMO, and L is LUMO)

According to Table 6, various transitions are responsible for the absorption behavior of the nanocones being studied. Not only the HOMO and LUMO, but also orbitals below HOMO or above LUMO are crucially involved in the most significant transitions. The percentage contribution of each critical transition in each nanostructure is detailed in Table 6.

Conclusion

BNNCs have received considerable interest in the medical field because of their distinct characteristics and possible uses. In this research four decorated BNNCs have been investigated to find efficient nanocarrier for anticancer drug, NU. The NLO response of nanostructure has been checked because of its crucial role in theranostic utilizations.

FMO analysis and considering global reactivity indices show that Mg-BNNC and Zn-BNNC are more reactive than Si-BNNC and Ni-BNNC. These species are capable for adsorption of drug agent, NU. Also, these nanocones show considerable NLO response. Mg-BNNC and Zn-BNNC show significant alterations in optical properties when they adsorb NU. This make trace of drug possible in medical applications. Different UV-vis absorption patterns in single form comparing with in complex, is another advantage of these nanocarriers.

MEP analysis and interaction energy consideration show that the Si-BNNC isn't a reliable candidate as a NU nanocarrier. It couldn't adsorb the drug molecule, effectively. Also, Si-BNNC shows the least NLO response among studied nanocones. It suffers the least variation in β and γ as a result of complexation with NU.

This study primarily focuses on theoretical assessments to elucidate the potential of BN nanocones as NLO-active nanocarriers for the nitrosourea anticancer drug. However, further experimental investigations are necessary to validate the findings of this article regarding stability under physiological conditions and to assess biocompatibility.

References

1. Steffy, A. D., Dhas, D. A., Joe, I. H., Gunasekaran, B., & Vinitha, G. (2024). An experimental and computational exploration on noncovalent interactions, spectroscopic and nonlinear optical properties of novel creatininium cyanoacetate single crystal. *Computational and Theoretical Chemistry, 1232*, 114445.
2. Kosar, N., Kanwal, S., Sajid, H., Ayub, K., Gilani, M. A., Ibrahim, K. E., ... & Mahmood, T. (2024). Frequency-dependent nonlinear optical response and refractive index investigation of lactone-derived thermochromic compounds. *Journal of Molecular Graphics and Modelling, 126*, 108646.
3. Jamshidi, A., & Biglari, Z. (2021). Electronic And Nonlinear Optical Features of Inorganic Ga12N12 Nanocage Decorated With Alkali Metals (Li, Na and K).
4. Forozmand, N., & Biglari, Z. (2021). Influence of lithiation on electro-optical properties of disk-like coronene molecule. *Physica E: Low-dimensional Systems and Nanostructures, 134*, 114838.
5. Bano, R., Nawaz, N., Arshad, M., Rauf, A., Mahmood, T., Ayub, K., ... & Gilani, M. A. (2024). Face specific superalkali doped corannulene complexes with significant electronic and nonlinear optical responses. *Optical and Quantum Electronics, 56*(2), 204.
6. Asif, A., Khan, M. U., Yaqoob, J., Mustafa, G., Ahmed, S., Alhokbany, N., ... & Janjua, M. R. S. A. (2023). Tuning nonlinear optical properties of tetracyclopentatetraphenylnene by superhalogens doping: Quantum chemical perspective of novel NLO materials for modern optoelectronic applications. *Materials Science and Engineering: B, 297,* 116763.
7. Lakhera, S., Rana, M., & Devlal, K. (2023). Influence of adsorption of gold and silver nanoclusters on structural, electronic, and nonlinear optical properties of pentacene-5, 12-dione: a DFT study. *Optical and Quantum Electronics, 55*(2), 178.
8. Baloach, R., Ayub, K., Mahmood, T., Asif, A., Tabassum, S., & Gilani, M. A. (2021). A new strategy of bi-alkali metal doping to design boron phosphide nanocages of high nonlinear optical response with better thermodynamic stability. *Journal of Inorganic and Organometallic Polymers and Materials, 31,* 3062-3076.
9. Rashid, M., Yaqoob, J., Khalil, N., Jamil, R., Khan, M. U., & Gilani, M. A. (2022). Nonlinear optical (NLO) response of boron phosphide nanosheet by alkali metals doping: A DFT study. *Materials Science in Semiconductor Processing, 151,* 107007.
10. Ishaq, M., Shehzad, R. A., Yaseen, M., Iqbal, S., Ayub, K., & Iqbal, J. (2021). DFT study of superhalogen-doped borophene with enhanced nonlinear optical properties. *Journal of Molecular Modeling, 27*(6), 188.
11. Asif, M., Sajid, H., Qureshi, S., Gilani, M. A., Mahmood, T., & Ayub, K. (2023). Boron-rich triphenylene COF based electrides having excellent nonlinear optical activity. *Materials Science in Semiconductor Processing, 160*, 107468.
12. Azaid, A., Alaqarbeh, M., Abram, T., Raftani, M., Kacimi, R., Khaddam, Y., ... & Bouachrine, M. (2024). D-π-A push-pull chromophores based on N, N-Diethylaniline as a donor for NLO applications: effects of structural modification of π-linkers. *Journal of Molecular Structure, 1295*, 136602.
13. Al Mahmud, A., Islam, M. M., Shek, M. M., Sheikh, M. C., & Miyatake, R. (2024). Theoretical investigations of pharmacological activities and solvent effect on structural and nonlinear optical properties of new methyl (E)-3-(2, 3, 4-trimethoxybenzylidene) dithiocarbazate. *Journal of Molecular Liquids, 395*, 123830.
14. Patil, P. S., & Sekar, N. (2024). Nonlinear optical properties of natural hydroxyanthraquinones studied using density functional theory (DFT) technique. *Journal of Photochemistry and Photobiology A: Chemistry, 446*, 115151.

15. Khalid, M., Maqsood, R., Shafiq, I., Baby, R., Asghar, M. A., Ahmed, S., ... & Braga, A. A. (2024). Theoretical approach towards benzodithiophene-based chromophores with extended acceptors for prediction of efficient nonlinear optical behaviour. *Arabian Journal for Science and Engineering, 49*(1), 339-359.
16. Dhawan, P., Saini, A., Grover, K., Goel, S., Tyagi, N., Kumar, P., ... & Yadav, H. (2024). A methodical investigation on the growth and characterization of a third-order nonlinear optical novel co-crystal of 8-hydroxyquinolinium phthalate: X-ray, Hirshfeld surface, optical, mechanical, thermal and DFT analysis. *Materials Research Bulletin, 169*, 112516.
17. Zhou, W., & Guo, S. P. (2024). Rational Design of Novel Promising Infrared Nonlinear Optical Materials: Structural Chemistry and Balanced Performances. *Accounts of Chemical Research, 57*(4), 648-660.
18. Zhang, J. X., Feng, P., Ran, M. Y., Wu, X. T., Lin, H., & Zhu, Q. L. (2024). Ga-based IR nonlinear optical materials: Synthesis, structures, and properties. *Coordination Chemistry Reviews, 502,* 215617.
19. Li, P. F., Hu, C. L., Mao, J. G., & Kong, F. (2024). A UV non-hydrogen pure selenite nonlinear optical material for achieving balanced properties through framework-optimized structural transformation. *Materials Horizons, 11*(7), 1704-1709.
20. Li, P. F., Gong, Y. P., Hu, C. L., Zhang, B., Mao, J. G., & Kong, F. (2024). Four UV Transparent Linear and Nonlinear Optical Materials Explored from Pure Selenite Compounds. *Advanced Optical Materials, 12*(2), 2301426.
21. Li, P. F., Gong, Y. P., Hu, C. L., Zhang, B., Mao, J. G., & Kong, F. (2024). Four UV Transparent Linear and Nonlinear Optical Materials Explored from Pure Selenite Compounds. *Advanced Optical Materials, 12*(2), 2301426.
22. Naeem, J., Bano, R., Ayub, K., Mahmood, T., Tabassum, S., Arooj, A., & Gilani, M. A. (2022). Assessment of alkali and alkaline earth metals doped cubanes as high-performance nonlinear optical materials by first-principles study. *Journal of Science: Advanced Materials and Devices, 7*(3), 100457.
23. Liu, Z. B., Zhou, Z. J., Li, Y., Li, Z. R., Wang, R., Li, Q. Z., ... & Sun, C. C. (2010). Push–pull electron effects of the complexant in a Li atom doped molecule with electride character: a new strategy to enhance the first hyperpolarizability. *Physical Chemistry Chemical Physics, 12*(35), 10562-10568.
24. Rafique, A., Maqbool, H., Shehzad, R. A., Bhatti, I. A., Ayub, K., Elmushyakhi, A., ... & Iqbal, J. (2023). DFT study of enhancement in nonlinear optical response of exohedrally and endohedrally alkaline earth metals (Be, Mg, Ca) doped adamanzane. *International Journal of Quantum Chemistry, 123*(6), e27060.
25. Njeumen, C. A., Ejuh, G. W., Assatse, Y. T., Kamsi, R. A. Y., Tekou, C. T. T., Zekeng, S. S., & Ndjaka, J. M. B. (2023). Application of carbon nanostructures toward acetylsalicylic acid adsorption: A comparison between fullerene ylide and graphene oxide by DFT calculations. *Computational and Theoretical Chemistry, 1227,* 114221.
26. Kamel, M., Saleh, E. A. M., Mohammadifard, K., Nigmatova, I. M., Bijlwan, S., Ramadan, M. F., & JM, A. H. (2023). Assessment of the adsorption mechanism of amantadine drug onto pristine, Si-and Ge-doped Al12N12, and Al12P12 nanocages: A comparative DFT study. *Materials Chemistry and Physics, 307*, 128116.
27. Saadh, M. J., Rasheed, Y. S., Sdiq, Z. M., Chandra, S., Lateef, S. R., Ghnim, Z. S., ... & Elmasry, Y. (2024). BN-biphenyl nanosheet as a potential drug carrier for 5-Fluorouracil: A DFT investigation. *Inorganic Chemistry Communications, 160*, 111857.
28. Rahimi, R., & Solimannejad, M. (2024). A novel pentagonal BCN monolayer for sensing and drug delivery of nitrosourea and hydroxyurea anticancer drugs: A DFT outlook. *Materials Science in Semiconductor Processing, 173,* 108109.
29. Kumar, R. A., Al-Otaibi, S. J., Mary, Y. S., Mary, Y. S., Acharjee, N., Thomas, R., ... & Leena, T. L. (2024). Surface adsorption of adenine on pristine and B/N/O/P-doped coronene as a biosensing substrate for DNA detection-DFT study. *Journal of Molecular Liquids, 393*, 123546.
30. Perveen, M., Noreen, L., Waqas, M., Mehmood, R. F., Iqbal, J., Manzoor, S., ... & Khera, R. A. (2023). A DFT approach for finding therapeutic potential of graphyne as a nanocarrier in the doxorubicin drug delivery to treat cancer. *Journal of Molecular Graphics and Modelling, 124*, 108537.
31. Rahimi, R., & Solimannejad, M. (2023). In silico study of B3O3 nanosheet as a disposable platform for sensing and delivery of carmustine anticancer drug. *Journal of Drug Delivery Science and Technology, 87*, 104828.
32. Edet, H. O., Louis, H., Gber, T. E., Idante, P. S., Egemonye, T. C., Ashishie, P. B., ... & Adeyinka, A. S. (2023). Heteroatoms (B, N, S) doped quantum dots as potential drug delivery system for isoniazid: insight from DFT, NCI, and QTAIM. *Heliyon, 9*(1).
33. Sartaj, A., Baboota, S., & Ali, J. (2021). Exploring the therapeutic potential of nanostructured lipid carrier approaches to tackling the inherent lacuna of chemotherapeutics and herbal drugs against breast cancer. *Journal of Drug Delivery Science and Technology, 63*, 102451.
34. Iqbal, A. J. B., Shahriar, R., & Zubair, A. (2024). First-principles study of a SiC nanosheet as an effective material for nitrosourea and carmustine anti-cancer drug delivery. *Nanoscale Advances, 6*(11), 2968-2979.
35. Al-Otaibi, J. S., Alamro, F. S., Almugrin, A. H., Mary, Y. S., Mary, Y. S., & Nair, D. S. R. (2024). Revealing patterns in Be12O12-metal nanocages as a nitrosourea drug delivery system: DFT, SERS, solvent effects and the role of periods and groups. *Computational and Theoretical Chemistry, 1236*, 114604.
36. Reichert, T., Vučićević, M., Hillman, P., Bleicher, M., Armaković, S. J., & Armaković, S. (2021). Sumanene as a delivery system for 5-fluorouracil drug–DFT, SAPT and MD study. *Journal of Molecular Liquids, 342*, 117526.
37. Rasheed, T., Nabeel, F., Raza, A., Bilal, M., & Iqbal, H. M. N. (2019). Biomimetic nanostructures/cues as drug delivery systems: a review. *Materials Today Chemistry, 13*, 147-157.
38. Augustine, S., Singh, J., Srivastava, M., Sharma, M., Das, A., & Malhotra, B. D. (2017). Recent advances in carbon based nanosystems for cancer theranostics. *Biomaterials science, 5*(5), 901-952.

39. Apebende, C. G., Ogunwale, G. J., Louis, H., Benjamin, I., Kadiri, M. T., Owen, A. E., & Manicum, A. L. E. (2023). Density functional theory (DFT) computation of pristine and metal-doped MC59 (M= Au, Hf, Hg, Ir) fullerenes as nitrosourea drug delivery systems. *Materials Science in Semiconductor Processing, 158,* 107362.
40. Asif, M., Sajid, H., Ayub, K., Gilani, M. A., Anwar, N., & Mahmood, T. (2023). Therapeutic potential of oxo-triarylmethyl (oxTAM) as a targeted drug delivery system for nitrosourea and fluorouracil anticancer drugs; A first principles insight. *Journal of Molecular Graphics and Modelling, 122*, 108469.
41. Gholami, A., Shakerzadeh, E., & Anota, E. C. (2023). A theoretical perspective on the adsorption performance of pristine and Metal-encapsulated B36N36 fullerenes toward the hydroxyurea and nitrosourea anticancer drugs. *Inorganic Chemistry Communications, 148,* 110326.
42. Zhang, L., Ye, Y. L., Li, X. H., Chen, J. H., & Sun, W. M. (2021). On the potential of all-boron fullerene B40 as a carrier for anti-cancer drug nitrosourea. *Journal of Molecular Liquids, 342,* 117533.
43. Khudhair, A. M., & Ben Ahmed, A. (2023). Anticancer drugs delivery and adsorption computations in pure and Stone–Wales defect armchair graphene nanoribbons. *Optical and Quantum Electronics, 55*(9), 812.
44. Ema, S. N., Khaleque, M. A., Ghosh, A., Piya, A. A., Habiba, U., & Shamim, S. U. D. (2021). Surface adsorption of nitrosourea on pristine and doped (Al, Ga and In) boron nitride nanosheets as anticancer drug carriers: the DFT and COSMO insights. *RSC advances, 11*(58), 36866-36883.
45. Ahmed, T., Rahman, M. A., Islam, R., Piya, A. A., & Shamim, S. U. D. (2022). Unravelling the adsorption performance of BN, AlN, GaN and InN 2D nanosheets towards the ciclopirox, 5-fluorouracil and nitrosourea for anticancer drug delivery motive: A DFT-D with QTAIM, PCM and COSMO investigations. *Computational and Theoretical Chemistry, 1214*, 113797.
46. Deng, S., Jiang, Q., Wang, Y., Lu, X., Zhu, Y., Zhang, Y., & Qiang, L. (2021). C4B32 nanocluster as a drug delivery system for nitrosourea anticancer drug: a first-principles perception. *Molecular Physics, 119*(3), e1808906.
47. Rahimi, R., & Solimannejad, M. (2020). BC3 graphene-like monolayer as a drug delivery system for nitrosourea anticancer drug: A first-principles perception. *Applied Surface Science, 525,* 146577.
48. Ahsan, F., Yar, M., Gulzar, A., & Ayub, K. (2023). Therapeutic potential of C2N as targeted drug delivery system for fluorouracil and nitrosourea to treat cancer: a theoretical study. *Journal of Nanostructure in Chemistry, 13*(1), 89-102.
49. Fahad, I. H., Sadoon, N., Kadhim, M. M., Alhussainy, A. A., Hachim, S. K., Abdulhussain, M. A., ... & Rheima, A. M. (2022). Potential of zinc carbide 2D monolayers as a new drug delivery system for nitrosourea (NU) anti-cancer drug. *Computational and Theoretical Chemistry, 1217*, 113927.
50. Mahal, R. K., Naser, S. M., Abdulhussain, M. A., Taha, A., Hachim, S. K., Abdullaha, S. A., ... & Taban, T. Z. (2022). First-principles studies on two-dimensional aluminum carbide as potential nanocarriers for drug delivery systems. *Inorganic Chemistry Communications, 145*, 110010.
51. Alkhalifah, M. A., Yar, M., Bayach, I., Sheikh, N. S., & Ayub, K. (2022). Covalent organic framework (C6N6) as a drug delivery platform for fluorouracil to treat cancerous cells: a DFT study. *Materials, 15*(21), 7425.
52. Hosseinian, A., Salary, M., Arshadi, S., Vessally, E., & Edjlali, L. (2018). The interaction of phosgene gas with different BN nanocones: DFT studies. *Solid State Communications, 269*, 23-27.
53. Saadh, M. J., Amin, A. H., Farhadiyan, S., Sadeghi, M. S., Shahrtash, S. A., Maaliw III, R. R., ... & Akhavan-Sigari, R. (2023). Sensing functions of an iron-doped boron nitride nanocone towards acetaminophen and its thio/thiol analogs: A DFT outlook. *Diamond and Related Materials, 133*, 109749.
54. Mohammadi, M. D., Abdullah, H. Y., Louis, H., & Mathias, G. E. (2022). 2D boron nitride material as a sensor for H2SiCl2. *Computational and Theoretical Chemistry, 1213*, 113742.
55. Anota, E. C. (2022). 2D boron nitride incorporating homonuclear boron bonds: stabilized in neutral, anionic and cationic charge. *SN Applied Sciences, 4*(11), 295.
56. Doroudi, Z., & Jalali Sarvestani, M. R. (2020). Boron nitride nanocone as an adsorbent and senor for Ampicillin: A Computational Study. *Chemical Review and Letters, 3*(3), 110-116.
57. Makiabadi, B., Zakarianezhad, M., Behjatmanesh-Ardakani, R., & Mousavi, S. H. (2024). Investigating the performance of BN nanotubes as drug delivery systems for Azacitidine and decitabine anti-cancer drugs: a theoretical study. *Computational and Theoretical Chemistry, 1231*, 114429.
58. Aiswarya, T., & Singh, K. K. (2024). Incrimination and impact on recovery times and effects of BN nanostructures on antineoplastic drug-electronic density study. *Journal of Molecular Modeling, 30*(11), 372.
59. Taheri, S. S., & Fakhrabadi, M. M. S. (2023). Elastic and inelastic behavior of boron nitride nanocones at finite strains. *Physics Letters A, 473*, 128812.
60. Fadlallah, M. M., Maarouf, A. A., & Soliman, K. A. (2019). Boron nitride nanocones template for adsorbing NO2 and SO2: an ab initio investigation. *Physica E: Low-dimensional Systems and Nanostructures, 113*, 188-193.
61. Khaki, N., Fosshat, S., Pourhakkak, P., Thanoon, R. D., Jalil, A. T., & Wu, L. (2022). Sensing of acetaminophen drug using Zn-doped boron nitride nanocones: a DFT inspection. *Applied Biochemistry and Biotechnology, 194*(6), 2481-2491.
62. Eaton, D. F. (1991). Nonlinear optical materials. *Science, 253*(5017), 281-287.
63. Al-Jouhani, S., Al-Azwari, R., Al-Shemari, S., Al-Anezi, R., Khasim, S., Mohamed, S., ... & Hamdalla, T. A. (2023). The effect of human serum albumin on ZIF-8 used in drug delivery: structural, linear and nonlinear optical properties. *Journal of Umm Al-Qura University for Applied Sciences, 9*(4), 521-528.
64. Gong, P., An, L., Tong, J., Liu, X., Liang, Z., & Li, J. (2022). Design of ADA-type organic third-order nonlinear optical materials based on benzodithiophene: a DFT study. *Nanomaterials, 12*(20), 3700.

65. Shafiq, S., Shehzad, R. A., Yaseen, M., Ayub, K., Ayub, A. R., Iqbal, J., ... & El-Bahy, Z. M. (2022). DFT study of OLi3 and MgF3 doped boron nitride with enhanced nonlinear optical behavior. *Journal of Molecular Structure, 1251*, 131934.
66. Souri, M. (2024). Ni-modified boron nitride nanocones as nonlinear optical active drug carriers, a DFT study. *Optical and Quantum Electronics, 56*(7), 1119.
67. Yaqoob, J., Mahmood, T., Ayub, K., Tabassum, S., Khan, A. F., Perveen, S., ... & Gilani, M. A. (2022). Optimized nonlinear optical (NLO) response of silicon carbide nanosheet by alkali metals doping: a DFT insight. The European Physical Journal Plus, 137(2), 233.
68. Zahid, S., Rasool, A., Ayub, A. R., Ayub, K., Iqbal, J., Al-Buriahi, M. S., ... & Somaily, H. H. (2022). Silver cluster doped graphyne (GY) with outstanding non-linear optical properties. RSC advances, 12(9), 5466-5482.
69. Shakerzadeh, E., Kazemimoghadam, F., & Anota, E. C. (2018). How Does Lithiation Affect Electro-Optical Features of Corannulene (C 20 H 10) and Quadrannulene (C 16 H 8) Buckybowls?. Journal of Electronic Materials, 47, 2348-2358.
70. Noudem, P., Fouejio, D., Mveme, C. D. D., Nya, F. T., & Zekeng, S. S. (2023). Electronic, nonlinear optical, UV–vis and NBO analysis of methyl methacrylate for optoelectronic and optical applications: DFT study and impact of conformation. Spectrochimica Acta Part A: Molecular and Biomolecular Spectroscopy, 303, 123267.
71. Guasch, L., Peach, M. L., & Nicklaus, M. C. (2015). Tautomerism of warfarin: combined chemoinformatics, quantum chemical, and NMR investigation. The Journal of organic chemistry, 80(20), 9900-9909.
72. Hasan, M. M., Das, A. C., Hossain, M. R., Hossain, M. K., Hossain, M. A., Neher, B., & Ahmed, F. (2022). The computational quantum mechanical investigation of the functionalized boron nitride nanocage as the smart carriers for favipiravir drug delivery: a DFT and QTAIM analysis. Journal of Biomolecular Structure and Dynamics, 40(23), 13190-13206.
73. Kumar, A., Al-Bahrani, M., Hossain, M. A., Mehedi, I. M., Iskanderani, A. I., Gavilán, J. C. O., & Ramaiah, G. B. (2023). Transition metal-functionalized porphyrin-like C70 fullerenes as sensors and adsorbents of formaldehyde-DFT, NBO, and QTAIM study. Inorganic Chemistry Communications, 153, 110883.
74. Pereira Silva, A. L., & Varela Júnior, J. D. J. G. (2022). Density functional theory study of Cu-modified B12N12 nanocage as a chemical sensor for carbon monoxide gas. Inorganic Chemistry, 62(5), 1926-1934.
75. Silva, A. L. P., Silva, A. C. A., & Júnior, J. D. J. G. V. (2022). Putrescine adsorption on pristine and Cu-decorated B12N12 nanocages: A density functional theory study. Computational and Theoretical Chemistry, 1215, 113836.
76. Zhang, L., Qi, Z. D., Ye, Y. L., Li, X. H., Chen, J. H., & Sun, W. M. (2021). DFT study on the adsorption of 5-fluorouracil on B 40, B 39 M, and M@ B 40 (M= Mg, Al, Si, Mn, Cu, Zn). RSC advances, 11(62), 39508-39517.
77. 77. Lee, H. J., Liu, S. W., Sulyok-Eiler, M., Harmat, V., Farkas, V., Bánóczi, Z., ... & Song, J. W. (2024). Neighbor effect on conformational spaces of alanine residue in azapeptides. Heliyon, 10(12).
78. O'boyle, N. M., Tenderholt, A. L., & Langner, K. M. (2008). Cclib: a library for package-independent computational chemistry algorithms. Journal of computational chemistry, 29(5), 839-845.
79. Souri, M. (2021). Theoretical investigation of the NLO properties of a series of (C5N) n bare graphene nanoribbons. Journal of Nanophotonics, 15(4), 046012-046012.
80. Souri, M. (2023). Density functional theory study of Ni-modified B12N12 nanocages as promising nonlinear optical materials. Chemical Physics Letters, 830, 140769.
81. Souri, M., & Mohammadi, A. K. (2017). Investigation of solvent effect on adenine-thymine base pair interaction. Journal of Molecular Liquids, 230, 169-174.
82. Maleki, A. (2022). Adsorption behavior of anti-cancer procarbazine on the surface of on pristine, Al-, Si-, and C-doped B24N24 fullerenes based on the density functional theory. Structural Chemistry, 33(2), 323-333.
83. Poiyamozhi, A., Sundaraganesan, N., Karabacak, M., Tanrıverdi, O., & Kurt, M. (2012). The spectroscopic (FTIR, FT-Raman, UV and NMR), first-order hyperpolarizability and HOMO–LUMO analysis of 4-amino-5-chloro-2-methoxybenzoic acid. Journal of Molecular Structure, 1024, 1-12.
84. El Mouhi, R., Slimi, A., Fitri, A., Benjelloun, A. T., ElKhattabi, S., Benzakour, M., ... & Kurban, M. (2022). DFT, DFTB and TD-DFT theoretical investigations of π-conjugated molecules based on thieno [2, 3-b] indole for dye-sensitized solar cell applications. Physica B: Condensed Matter, 636, 413850.
85. El Mouhi, R., Daoui, O., Fitri, A., Benjelloun, A. T., El Khattabi, S., Benzakour, M., ... & Kurban, M. (2023). A strategy to enhance V OC of π-conjugated molecules based on thieno [2, 3-b] indole for applications in bulk heterojunction organic solar cells using DFT, TD-DFT, and 3D-QSPR modeling studies. New Journal of Chemistry, 47(2), 812-827.
86. Deb, J., Paul, D., & Sarkar, U. (2020). Density functional theory investigation of nonlinear optical properties of T-graphene quantum dots. The Journal of Physical Chemistry A, 124(7), 1312-1320.
87. Khan, M. U., Janjua, M. R. S. A., Yaqoob, J., Hussain, R., Khalid, M., Syed, A., ... & Zaghloul, N. S. (2023). First theoretical framework of superalkali metals [M3X (M= Li, Na, k; X= O, S, F, N)] doped all-boron B38 nanocluster: A promising class of nonlinear optical materials for optoelectronic applications. Journal of Photochemistry and Photobiology A: Chemistry, 440, 114667.
88. Tu, X., Xu, H., Li, C., Liu, X., Fan, G., & Sun, W. (2021). Adsorption performance of boron nitride nanomaterials as effective drug delivery carriers for anticancer drugs based on density functional theory. Computational and Theoretical Chemistry, 1203, 113360.
89. Hosseinzadeh, E., Foroumadi, A., & Firoozpour, L. (2023). A DFT study on the transition metal doped BN and AlN nanocages as a drug delivery vehicle for the cladribine drug. Journal of Molecular Liquids, 374, 121262.